

# Chapter 7

## An Integrated Regional and On-Site Earthquake Early Warning System for Southern Italy: Concepts, Methodologies and Performances

A. Zollo, S. Colombelli, L. Elia, A. Emolo, G. Festa, G. Iannaccone, C. Martino and P. Gasparini

**Abstract** We present an approach to Earthquake Early Warning for Southern Italy that integrates regional and on-site systems. The regional approach is based on the PRobabilistic and Evolutionary early warning SysTEM (PRESTo) software platform. PRESTo processes 3-components acceleration data streams and provides a peak ground-motion prediction at target sites based on earthquake location and magnitude computed from P-wave analysis at few stations in the source vicinity. On the other hand, the on-site system is based on the real-time measurement of peak displacement and dominant period, on a 3 s P-wave time-window. These values are compared to thresholds, set for a minimum magnitude 6 and instrumental intensity VII, derived from empirical regression analyses on strong-motion data. Here we present an overview of the system and describe the algorithms implemented in the PRESTo platform. We also show some case-studies and propose a robust methodology to evaluate the performance of this Early Warning System.

### 7.1 Introduction

The concept of Earthquake Early Warning System (EWS) today is becoming more and more popular in the seismological community, especially in the most active seismic regions of the world. EEW means the rapid detection of an ongoing earthquake and the broadcasting of a warning in a target area, before the arrival of the destructive waves. Earthquake Early Warning Systems experienced a sudden improvement

---

A. Zollo (✉), S. Colombelli, L. Elia, A. Emolo, G. Festa, C. Martino, P. Gasparini  
Department of Physics, University of Naples Federico II, Naples, Italy  
e-mail: aldo.zollo@unina.it

G. Iannaccone  
Osservatorio Vesuviano, INGV, Naples, Italy

L. Elia, C. Martino, P. Gasparini  
AMRA Scarl, Naples, Italy

and a wide diffusion in many active seismic regions of the world in the last three decades. They are currently operating in Japan (Nakamura 1984, 1988; Odaka et al. 2003; Horiuchi et al. 2005), Taiwan (Wu and Teng 2002; Wu and Zhao 2006), and Mexico (Espinosa-Aranda et al. 2009). Many other systems are under development and testing in other regions of the world such as California (Allen and Kanamori 2003; Allen et al. 2009a,b; Böse et al. 2009), Turkey (Alcik et al. 2009), Romania (Böse et al. 2007), and China (Peng et al. 2011). In southern Italy the early warning system PRESTo (Probabilistic and Evolutionary early warning SysTem) (Satriano et al. 2010) is under testing since December 2009. It is currently used to monitor the Apenninic fault system and to detect small-to-moderate size events in the area where the  $M_W$  6.9, 1980 Irpinia earthquake occurred (Zollo et al. 2009a; Zollo 2009b; Iannaccone 2010).

Most of existing EEWS essentially operate in two different configurations, the “regional” (or network-based) and the “on-site” (or station-based), depending on the source-to-site distance and on the geometry of the considered network with respect to the source area. The regional configuration is generally adopted when the network is deployed in the source area, while the targets to be protected are far away from it. In this approach, the early portion of recorded signals is used to rapidly evaluate the source parameters (essentially, event location and magnitude) and to predict a ground-motion intensity measure (e.g., Peak Ground Velocity, PGV, and/or Peak Ground Acceleration, PGA) at distant sites, through empirical Ground Motion Prediction Equations (GMPE). As data are acquired by the network, the initial estimations are updated, providing a continuously refined information about the earthquake parameters and ground shaking prediction at target sites. Given the source-to-site distance, the “lead-time” (i.e., the time between the alert issue and the arrival of damaging waves at the target site) can be relatively long in a regional configuration, although the prediction of the shaking at distant sites may be affected by large uncertainties due to the use of empirical predictive relationships.

The on-site approach, instead, is generally used when the sites to be protected are close to the source area. In this configuration the early portion of recorded P-wave signals is used to predict the ensuing peak ground-motion at the same site and to provide a local alert level, based on the combination of Early Warning (EW) parameters (such as P-wave peak displacement and/or predominant period). The main advantage of such an approach is that the alert for an impending earthquake at the target site is issued based on a local measurement of P-wave ground motion, avoiding the use of empirical predictive laws and bypassing the estimation of earthquake location and magnitude, which might be affected by large uncertainties in a real-time analysis.

The new idea for EEWS is the integration of the two approaches, which allows to get accurate estimations of earthquake parameters, reliable prediction of the expected ground motion and quite large lead times. The integrated approach, recently proposed by Zollo et al. (2010), is essentially based on three key-elements: (i) the definition of a local alert level from the combination of the initial Peak Displacement ( $P_d$ ) and the average dominant period ( $\tau_c$ ); (ii) the use of the initial peak displacement as a proxy for the Peak Ground Velocity; (iii) the real-time mapping of a Potential Damage Zone (PDZ). The integrated approach has been off-line tested for the 2009,

$M_W$  6.3 L'Aquila (Central Italy) earthquake and ten Japanese large earthquakes Colombelli et al. (2012). Recently, the method has been also implemented in the PRESTo software platform, and is currently under testing in southern Italy using data streaming of small-to-moderate events from the Irpinia Seismic Network (ISNet).

In the present paper we describe the PRESTo software platform, with a special focus on the methodologies and on the performance evaluation for the system.

## 7.2 The PRESTo Software Platform

PRobabilistic and Evolutionary early warning SysTEM (PRESTo) (Satriano et al. 2010) is a software platform for EEW that integrates recently developed algorithms for real-time earthquake location, magnitude estimation and damage assessment into a highly configurable and easily portable package. The system is under active experimentation in southern Italy on the Irpinia Seismic Network (ISNet) (Iannaccone 2010), which is deployed around the seismogenic area where the 1980,  $M_W$  6.9 Irpinia earthquake occurred, and that is expected to produce a large earthquake within the next 20 years.

PRESTo continuously processes the live streams of 3-components acceleration data from the stations for P-waves arrival detection and, while an earthquake is occurring, promptly performs the event detection, location, magnitude estimation, damage zone assessment and peak ground-motion prediction at target sites. The earthquake location uses an evolutionary real-time technique based on an Equal Differential Time (EDT) formulation, and a probabilistic approach for defining the hypocenter (Satriano et al. 2008). This algorithm, at each time step, relies on both the information from triggered arrivals and not-yet-triggered stations. The latter information enable the algorithm to rapidly constrain the most likely location area in the first few seconds of the P-wave propagation. Magnitude estimation exploits an empirical relationship that correlates the final event magnitude with the logarithm of the filtered peak ground-displacements, measured over the first  $2 \div 4$  s of signal starting at the detected P-wave arrival and the estimated S-wave arrival (Lancieri and Zollo 2008). The peak ground-motion parameters (PGA, PGV) at a given distance can be estimated from location and magnitude using region specific Ground Motion Prediction Equations (e.g., Emolo et al. 2011 for low-magnitude earthquakes; Akkar and Bommer 2007 for moderate-to-large magnitude events). The evolutionary estimates of source parameters and ground shaking at target sites, and their respective uncertainties, are sent as alarm messages to vulnerable structures and can reach them before the destructive waves arrive, enabling the recipients to initiate automatic safety procedures. PRESTo is designed to handle both low-magnitude and moderate-to-large earthquakes, by using two different sets of parameters for its algorithms at the same time (e.g., signal filters, regression laws, thresholds). This allows to test the real-time behavior of the system both for the low-magnitude seismicity, currently occurring in the Irpinia region, that is recorded by the ISNet network, and, at the same time, to perform Early Warning for eventual energetic earthquakes. PRESTo

has been under continuous real-time testing during the past two years (2010–2011) using data streaming from the ISNet stations, and has produced a bulletin of more than a hundred low-magnitude events (<http://isnet.fisica.unina.it>). Meanwhile, due to the unavailability of large magnitude events recorded at ISNet, PRESTo has been tested off-line, by playing-back in the system both real and synthetic seismograms for moderate-to-large events occurred in Italy and elsewhere (Satriano et al. 2010).

When a dense seismic network is deployed in the fault area, PRESTo can produce reliable estimates of earthquake location and size within 5–6 s from the event origin time, and a stable solution is generally reached within 10 s from it.

After analyzing strong motion data from modern accelerometric networks deployed in Japan, Taiwan and Italy, we recently integrated the regional approach with a threshold-based EW method that allows, in the very first seconds after the occurrence of a moderate-to-large seismic event, to map the most probable damaged zone which is a relevant information for the efficient planning of the rescue operations in the immediate post-event emergency phase. The method is based on the real-time measurement, at near-source stations located at increasing distances from the earthquake epicenter, of two parameters evaluated over a three-seconds window after the P-wave arrival: the peak displacement ( $P_d$ ) and the predominant period ( $\tau_c$ ) given by

$$\tau_c = 2n \sqrt{\frac{\int_0^{t_0} [u(t)]^2 dt}{\int_0^{t_0} [v(t)]^2 dt}} \quad (7.1)$$

where  $u$  is ground displacement and  $v$  is velocity on a short 3 s time-window of P-waves signal on the vertical component. The measured values are compared to threshold values, set for a minimum magnitude of 6 and instrumental intensity VII, based on the empirical regression analysis of strong motion data (Colombelli et al. 2012). At each recording site, an alert level is assigned based on a decision table with four alert levels according to the  $P_d$  and  $\tau_c$  values. Given the real-time, evolutionary estimation of earthquake location from first-P arrivals, the method provides an estimation of the extent of the potential damage zone as inferred from continuously updated averages of the period parameter and from mapping of the alert levels determined at the near-source accelerometer stations.

Concerning implementation details, PRESTo is a stand-alone executable written in C++, a programming language that provides optimal speed performance (a key element for an early-warning system) without sacrificing the code expressiveness, thanks to its object-oriented nature. The code is easily portable to different operating systems (Windows, Linux and Mac OS X), thanks to the SDL library (Simple Direct-Media Layer), used for abstracting low-level operations, and the OpenGL libraries, a de facto standard for scientific and interactive visualization. The software is organized into a main thread that implements the core processing procedures activated during an earthquake, and some additional processing threads that handle the continuous tasks, such as waveforms acquisition and their processing. A block diagram of the system and its inputs and outputs is reported in Fig. 7.1. The main tasks performed by the system are described hereinafter.

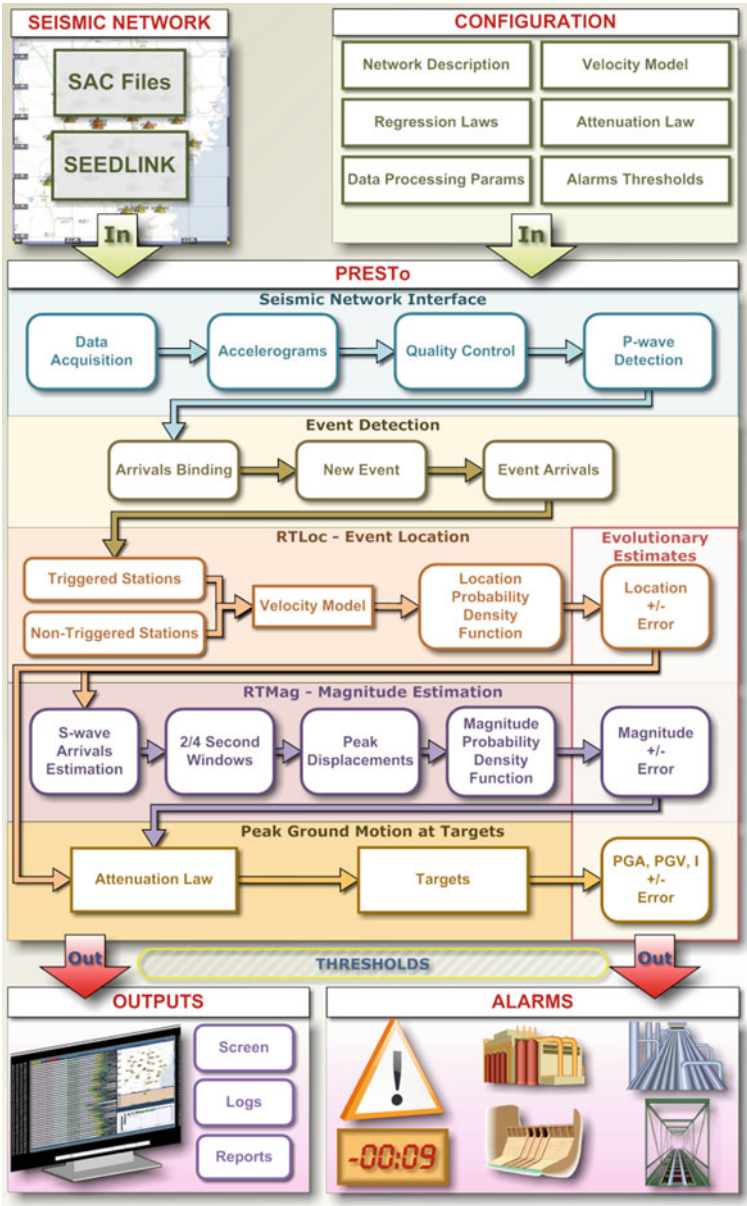


**Fig. 7.1** Block diagram of the PRESTo early warning system (*middle*) showing its inner components and the data exchange among them. The data-flow starts with inputs to the system (*top*) and ends with its outputs (*bottom*)

In real-time mode, ground acceleration from three components (or optionally from just the vertical component) is acquired from the stations via the SeedLink protocol. This is a robust and widely used protocol for waveform data transmission in seismology, and is implemented using the official libSlink library. Conversely, in simulation mode the waveforms recorded during a past earthquake (or synthetic waveforms produced for historical events), can be played-back in the system reading files in SAC format (Goldstein et al. 2003). In the latter case the streams of 1 s SeedLink packets are simulated, with the optional feature of also producing random communication delays and data gaps for a more realistic test. For each station, a thread running concurrently with the rest of the program performs the acquisition and automatic phase picking.

Incoming acceleration packets are processed for automatic phases picking by the Filter Picker (FP) algorithm developed by Lomax et al. (2012), which is based on the same basic concepts used in the Baer and Kradolfer's picker (Baer and Kradolfer 1987) and the Allen's picker (Allen 1978, 1982). FP is designed so that it operates stably on continuous, real-time, broad-band signals, and avoiding excessive picking during large events. It is able to analyze only the new packets of data, as it retains memory of past computations, rather than having to re-process a larger waveform buffer every time. Picks are produced as soon as the arrival waveform is available, making it especially suitable for an EW application. Furthermore, the picker is easily configurable with only five parameters (three of which can use defaults based on the sampling rate only if needed).

For all detected P-waves arrivals an on-site (i.e., local to the station) threshold based alert level is computed, telling whether to expect local and/or remote damage. The alert level (0–3) is computed by measuring the peak displacement  $P_d$  and predominant period  $\tau_c$  (Eq. 7.1), and comparing their values with threshold values. The default thresholds have been chosen in order to have the maximum alert level (level 3) for an earthquake characterized by a predicted magnitude  $M$  larger than 6 and an Instrumental Intensity ( $I_{MM}$ ) larger than VII. The alert level at each station is based solely on data recorded at that site, and is independent of the information provided by other stations and/or from the earthquake detection performed by the regional EW algorithms. In an integrated regional/on-site approach, an instrumental intensity map can be computed starting from a region-wide grid of expected PGVs. This parameter is predicted at stations using a correlation between the on-site  $P_d$  measured on a short time window and PGV, while elsewhere it is provided by the regional system through the estimation of the earthquake source parameters and using a GMPE. PGV is correlated to  $I_{MM}$  that in turn is correlated to the expected damage so that, through interpolation, a region-wide Potential Damaged Zone can be provided in a few seconds after the earthquake origin time.

The main thread, which runs in parallel with the acquisition threads, keeps a list of the last P-waves picks as well as detected earthquakes, in order to perform the Early Warning on more than one earthquake. A new event is declared when arrivals at a fixed number of stations are detected in a short coincidence time window. Subsequent picks at further stations are associated to the latest quake if they fall within the

association time window, or they are kept in a list of non-associated picks for the possible declaration of new earthquakes.

The probabilistic earthquake location of recent earthquakes is updated using the RTLoc algorithm (Satriano et al. 2008), if either new picks have been associated to the event, or more than a second has passed from the previous location estimate. The most probable hypocenter, origin time and covariance matrix (uncertainty ellipsoid) are computed based on the velocity model of the geographic area, P-waves arrival times at stations, non-triggered stations and current time. The velocity model is provided in two 3D grids per station, holding the travel times from each point of the location grid to the station (one grid for P-waves and one for S-waves).

Magnitude is continually estimated for still live earthquakes that were successfully located. The peak displacements are measured at each station associated to the event, as soon as waveform data are available in a short time window ( $2 \div 4$  s) after the detected P-waves arrival and theoretical S-waves arrival. Each time window provides a Gaussian-like magnitude Probability Density Function for the station, with mean value given by

$$\frac{\log P_d - A - C \log \left( \frac{R}{10} \right)}{B} \quad (7.2)$$

where  $R$  is the hypocentral distance in km,  $P_d$  is the filtered peak displacement in meters and  $A$ ,  $B$  and  $C$  are coefficients that depend on the signal window. The earthquake magnitude probability distribution is obtained, assuming a Bayesian approach, by multiplying together the distributions for all time windows and stations, with an *a priori* distribution corresponding to the Gutenberg-Richter law. This provides both a most likely magnitude (peak of the distribution) and uncertainty (magnitude range where the integral of the distribution rises from 5 to 95 %). If the resulting magnitude is below a threshold (i.e., a low-magnitude event was detected) the magnitude is recomputed using different filters to obtain the displacement. For this reason it is possible to test the behavior of the system on low-magnitude events, while at the same time performing Early Warning for moderate-to-large earthquakes.

Using magnitude and location from the previous steps, the peak velocity and acceleration are estimated at stations (to compare with measured values) and targets, through attenuation laws whose coefficients can be user-specified. The lead-time at each target site, i.e., the seconds remaining before the estimated S-waves arrival there, is also computed. However, the actual lead-time available to perform automatic safety procedures at targets is expected to be larger than that estimated by the system, considering that the peak ground-motion due to S-waves is expected to occur later than the S-waves arrival time.

Alarm messages are sent over the internet to remote target sites. These are short User Datagram Protocol (UDP) packets that contain the most up-to-date estimated source parameters and uncertainties, the peak ground shaking expected at the recipient target, and the remaining seconds before the arrival of destructive waves (S-waves). The average measured  $P_d$  and  $\tau_c$  at the stations are also provided. The UDP transport layer has been chosen since alarms are short, stream-like (e.g., the most recent message supersedes previous ones) and need to be delivered as fast as

possible, that is what UDP is designed for. In addition to “earthquake” messages, “heart-beat” messages are also continuously sent to targets (e.g., every few seconds) to signal the working condition of the EWS and communication lines. As a last step, the final estimates of the earthquake source parameters are sent as cell phone text message to a distribution list, as well as via e-mail (in this case also attaching a short log and a screenshot), and the PRESTo bulletin is updated.

### 7.3 Methodology

With the purpose to build a powerful tool for end-users, the PRESTo software platform has been conceived to be a fully adaptable system. The large number of configuration parameters and the different accepted input/output data format make it suitable to various seismogenic regions and network configurations. At present PRESTo is running in two different configurations. On the one hand it runs as a standard regional system, providing earthquake location, magnitude and regional alert notification; on the other hand it works as a On-site/Threshold-based approach, providing the local alert levels as a common single-station system. Both configurations are currently under testing at ISNet network; the next step will be the integration of the two approaches for the construction of a complete system, capable of providing several outputs and information about the earthquake underway.

In its original development, the PRESTo software platform has been conceived to be a regional system using the stations of ISNet network. The system is aimed at the real-time monitoring of the Campania Lucania Apennine (Southern Italy) and at providing a warning in specific target area of the Campania region (e.g., the city of Naples, about 100 km away from the source area). We have described in the previous section how both modalities are implemented in the PRESTo system. Hereinafter we are going to describe with some detail the theory that underlies the threshold-based configuration, referring to the articles by Zollo et al. (2010) and Colombelli et al. (2012) for further information.

The “threshold-based” method is essentially based on the real-time, joint measurement of initial peak displacement ( $P_d$ ) and average period ( $\tau_c$ ) (Wu and Kanamori 2005, 2008) in a 3 s window after the P-wave arrival time. In this approach, the initial peak displacement is used as a proxy for the Peak Ground Velocity in order to get a real-time estimation of the Potential Damage Area.

Based on the analysis of strong-motion data from different seismic regions of the world, (Zollo et al. 2010) derived the regression relationship between the initial peak displacement  $P_d$  and the Peak Ground Velocity. Measuring  $P_d$  in centimeters and PGV in centimeters per seconds they found:

$$\log(PGV) = 0.73(\pm 0.01) \cdot \log(P_d) + 1.30(\pm 0.02). \quad (7.3)$$

The period parameter, ( $\tau_c$ , Eq. 7.1), is instead used to estimate the earthquake magnitude  $M$ . Measuring  $\tau_c$  in seconds and through a best-fit weighted regression



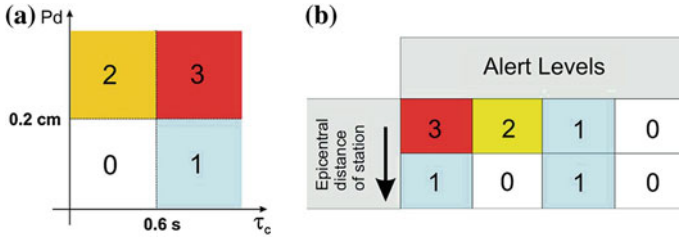


**Fig. 7.2** Alert levels and threshold values for observed early warning parameters (after Zollo et al. 2010). **a**  $P_d$  versus  $\tau_c$  diagram showing the chosen threshold values and the regions delimiting the different alert levels: level 3 means damage expected nearby and far away from the station; level 2 means damage expected only nearby the station; level 1 means damage expected only far away from the station; level 0 means no expected damage. **b** Expected variation of alert levels as a function of the epicentral distance: the allowed transitions between alert levels are from 3 to 1 and from 2 to 0

line on average binned data ( $\Delta M = 0.3$ ) with the same data set used before, (Zollo et al. 2010) found:

$$\log(\tau_c) = 0.21(\pm 0.01) \cdot M - 1.19(\pm 0.08). \tag{7.4}$$

In a standard attenuation relationship, the peak amplitude depends, at the first order, on the hypocentral distance ( $R$ ) and on the earthquake magnitude, thus, given the dependency of average period on the earthquake magnitude, Eqs. 7.3 and 7.4 have been combined in order to derive an empirical relationship among  $P_d$ ,  $\tau_c$  and hypocentral distance  $R$ . A multivariate linear regression analysis provided the following equation:

$$\log(P_d) = 1.93(\pm 0.03) \cdot \log(\tau_c) - 1.23(\pm 0.09) \cdot \log(R) + 0.6(\pm 0.1) \tag{7.5}$$

where  $R$  is measured in kilometers,  $\tau_c$  in seconds,  $P_d$  in centimeters.

As usual in a common on-site system, the two EW parameters are measured along the first 3 s of signal after the P-wave arrival time. The measured values of  $P_d$  and  $\tau_c$  are then compared to threshold values and a local alert level is assigned at each recording site, based on a decision table. Four alert levels (0, 1, 2 and 3) have been defined based on the combination of  $P_d$  and  $\tau_c$  at a given site; the threshold values have been set according to Eqs. 7.3 and 7.4 and correspond to a minimum magnitude  $M = 6$  (from the  $\tau_c$  versus  $M$  equation) and to an instrumental intensity  $I_{MM} = VII$  from the  $P_d$  versus PGV equation, assuming that the peak ground velocity could provide the instrumental intensity through the relationship of (Wald et al. 1999).

The alert level scheme comes from an original idea of (Wu and Kanamori 2005) and can be interpreted in terms of potential damaging effects nearby the recording station and far away from it. For example, following the scheme of Fig. 7.2, the maximum alert level (level 3, i.e.  $\tau_c \geq 0.6 \text{ s}$  and  $P_d \geq 0.2 \text{ cm}$ ) corresponds to an earthquake with predicted magnitude  $M \geq 6$  and with an expected instrumental

intensity  $I_{MM} \geq VII$ . This means that the earthquake is likely to have a large size and to be located close to the recording site. Thus, we expect a high level of damage either nearby and far away from the recording station. On the contrary, in case of a recorded alert level equal to 0 (i.e.,  $\tau_c < 0.6$  s and  $P_d < 0.2$  cm), the event is likely to be small and far from the site, thus no damage is expected either close or far away from the station. Analogous considerations can be done for the alert levels 1 and 2.

The “threshold-based” integrated method combines the use of a regional network with the single-station approach, using the scheme discussed in the following.

As soon as a station has been triggered by an earthquake, a preliminary location is obtained by using the real-time location technique implemented in the RTLoc code of (Satriano et al. 2008). As soon as 3 s of P-wave signal are available,  $P_d$  and  $\tau_c$  are measured at the triggered station and a local alert level is assigned based in their combination. The whole area of interest (i.e., the area covered by stations and the target area) is then divided into cells and Eq. 7.5 is used to predict peak displacement values at each node of the grid so to fill the gaps where the measurements are not yet available (Colombelli et al. 2012). Then, measured and predicted  $P_d$  values are interpolated and the Potential Damage Zone is delimited by the isoline corresponding to  $P_d = 0.2$  cm, which represents the threshold level on the initial peak displacement.

This routine is repeated every second so to update the PDZ. As other stations are triggered and 3 s of P-wave signal are available,  $P_d$  and  $\tau_c$  are measured and further local alert levels are assigned. Meanwhile, the event location is refined by using all the available P-picks and more data are used for the interpolation procedure.

## 7.4 Application and Performances

In this section we describe and discuss two different strategies for a quantitative assessment of the system performances: the former is relative to the regional configuration while the latter refers to the on-site methodology.

### 7.4.1 Regional Configuration

PRESTo is continuously running on real-time data streaming from 31 stations of the Irpinia Seismic Network. The performance of the regional approach to EEW implemented in PRESTo was evaluated by comparing the real magnitude and origin time of each event from the manually revised ISNet Bulletin (<http://isnet.fisica.unina.it>) to the final estimates obtained in real time by PRESTo.

We evaluated the performance by counting the total number of detected events and the missed and false alarms, using 162 microevents ( $0.5 \leq M \leq 3.7$ ) recorded from 2009/12/21 to 2011/11/15. Successful, missed and false alarms are defined according to the criteria provided in the Table 7.1.

**Table 7.1** Criteria adopted to distinguish among successful, missed and false alarms in testing the performance of the PRESTo system in the regional configuration

Successful alarm	An event for which the differences in magnitude ( $\Delta M$ ) and origin time ( $\Delta OT$ ) with respect to the real values are small: $\Delta M \leq 1$ and $\Delta OT \leq 15$ s
Missed alarm	An event with $M \geq 2.5$ that is not automatically detected
False alarm	A false event (for instance, a storm) that is declared by PRESTo

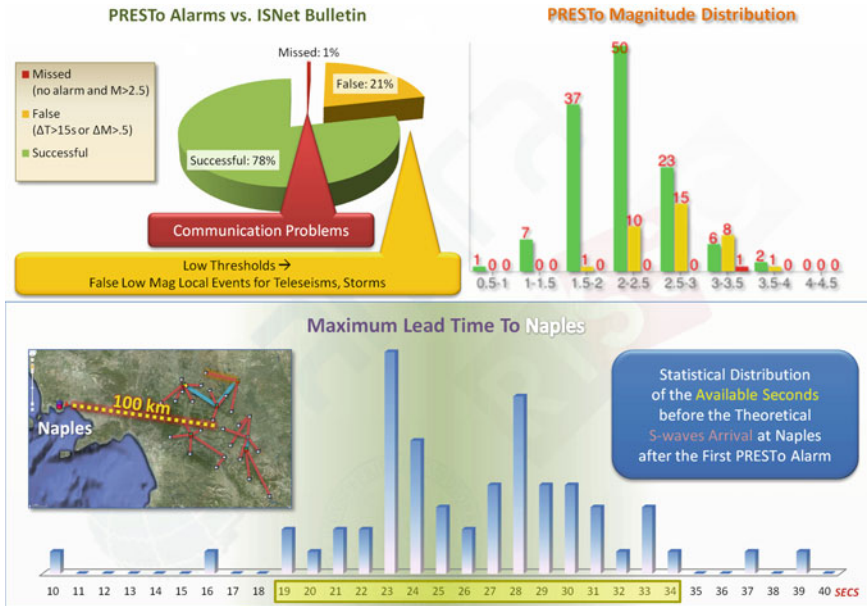


**Fig. 7.3** Statistics for the real-time performance of PRESTo in the regional configuration, performed on the low-magnitude seismicity recorded by the ISNet network ( $0.5 \leq M \leq 3.7$ ). *Top-left* percentages of successful, missed and false alarm based on the discrepancy with the manually revised ISNet Bulletin. *Top-right* distribution of magnitude estimates for each class of alarm. *Bottom* distribution of the seconds available to the city of Naples for events detected by PRESTo: interval from the very first PRESTo alarm to the arrival of S-waves

The statistics derived from the analysis are shown in Fig. 7.3. We have to stress that the (small number of) missed alarms are caused by communication problems among stations. False alarms (about one fifth of the analyzed events) are essentially associated with storms, that in case of adverse weather conditions may be declared as seismic events, and with regional events that are incorrectly declared as local events since the hypocentral searching is restricted to the region covered by the location grid encompassing ISNet. In the same figure we also represented the Maximum Lead Times for the city of Naples (located about 100 km far from the network) i.e.,

the difference between the time at which the first alert is issued and the theoretical S-waves arrival time at the city center.

As a further application, we studied off-line the performance of PRESTo for the L'Aquila earthquake that occurred in central Italy on 6th April 2009 ( $M_L$  5.9,  $M_W$  6.3). The seismic event was caused by a rupture produced along a fault of about 17 km in length, oriented along the Apenninic direction, and had an hypocentral depth of about 8 km (Cirella et al. 2009; Maercklin et al. 2011). It caused hundreds of victims and considerable damage to buildings, with the city of L'Aquila, at about 6 km away from the epicenter being particularly struck. We simulated this earthquake in PRESTo by playing-back three-component accelerograms recorded by the 18 stations of the National Accelerometric Network (RAN) closest to the epicenter. The employed velocity model can be found in Bagh et al. (2007). It is characterized by a  $V_P/V_S$  ratio equal to 1.83.

Figure 7.4 shows two screenshots of PRESTo during the simulation: in the top panel is reported the second alarm sent by the system that is the first alarm issued characterized by low uncertainties, while in the bottom panel the final estimates are shown.

A detailed study of the temporal evolution of inputs and outputs is shown in Fig. 7.5. The first estimate of location and magnitude was available 5.6 s after the actual origin time, which is just 2.1 s after the first P-waves arrival at station AQV. It is a very short interval, considering that before being able to estimate the earthquake magnitude, it is necessary to wait for the triggering of few stations in a short time frame in order to locate the hypocenter, and that at least 2 s of signal of either S- or P-waves is needed to be available. The promptness of PRESTo to send the first alert is then to be attributed to the high density of stations in near proximity of the epicenter (AQV, AQG, AQK, GSA, MTR, ANT and FMG). The very first magnitude estimate is affected by a large uncertainty as it basically relies on a single station, GSA. The other stations are in fact too close to the epicenter so that even the shortest 2 s P-waves window can't be used due to overlapping with the S-waves window. Therefore, 2 further seconds after the S-waves arrival at these stations need to elapse before they can contribute to improve the magnitude estimation. After just one second from the first alarm a good estimate of the source parameters is already available, i.e. it is in good agreement with the actual values and affected by a small uncertainty.

The maximum lead-times, i.e. relative to the very first estimate that is provided, for two remote sites to protect are: 10.5 s for the city of Teramo, and 22.6 s for Rome, minus 1 s in a more reasonable scenario whereby the recipients wait for a smaller uncertainty, which is indeed provided by the second alert. These are the best possible results given the requisites of the employed methodology. Figure 7.6 contains a plot of measured peak ground velocities at the stations (PGV) as a function of the estimated lead-times. The lead-times are conservative as they were calculated from the second alarm issued by PRESTo. Finally, the PGV estimates provided by PRESTo at the RAN stations are almost always consistent with the measured values, or with a discrepancy that does not exceed 0.5 logarithmic units.



**Fig. 7.4** Screen shots of PRESTo during the simulation of the 2009, ML 5.9, L'Aquila earthquake. *Top* the first estimates of the earthquake source parameters that are affected by a low uncertainty are provided about 7s after the origin time. *Bottom* the earthquake has been processed for some seconds and the estimates have converged to the final values. This screen shot shows the complete picture of inputs and outputs

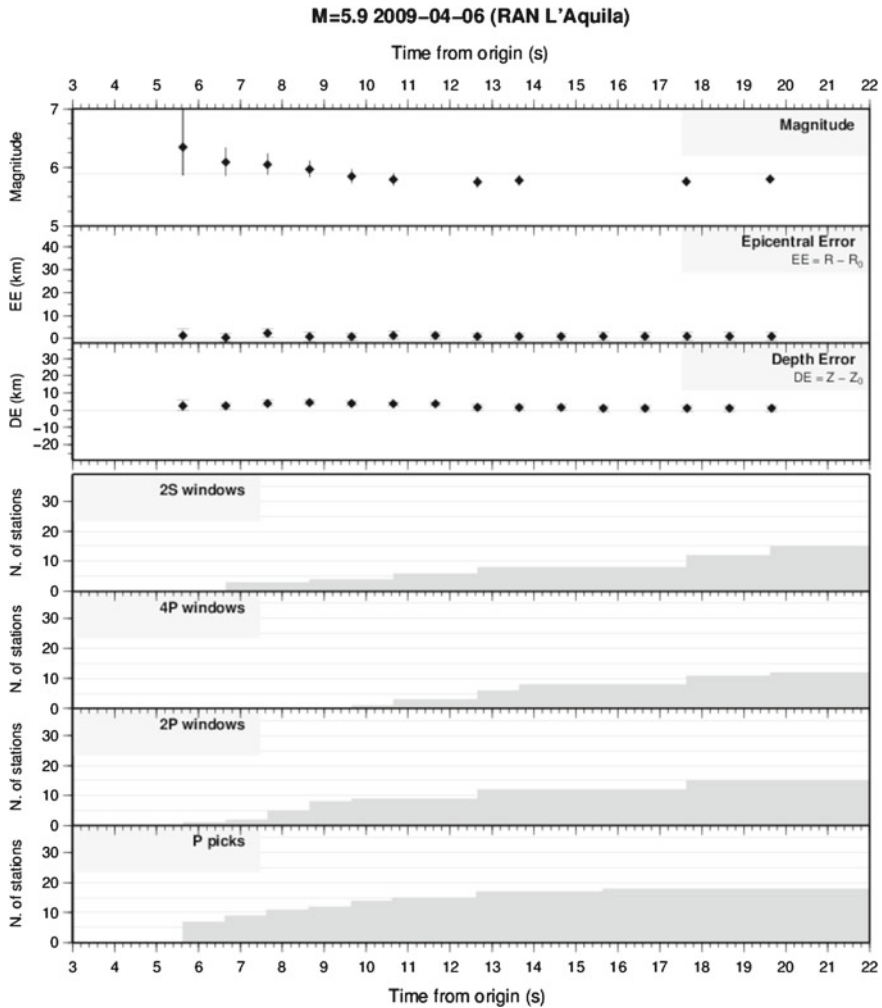


**Fig. 7.5** Play-back in PRESTo of the 2009 L'Aquila earthquake: temporal evolution of input data (*bottom* cumulative number of signal time windows and arrival times) and of PRESTo estimates (*top* magnitude, epicenter, depth). The latter are compared with the reference values (from the INGV Bulletin available at <http://cnt.rm.ingv.it>)

### 7.4.2 On-Site Methodology

The “threshold-based” on-site methodology has been tested off-line on ten Japanese strong earthquakes ( $M > 6$ ) for a total number of 1,341 records.

A first qualitative analysis of results can be obtained from the visual comparison of the rapidly predicted potential damage zone and the observed ground shaking (or intensity) distribution. The real-time PDZ (i.e., the area delimited by the isoline

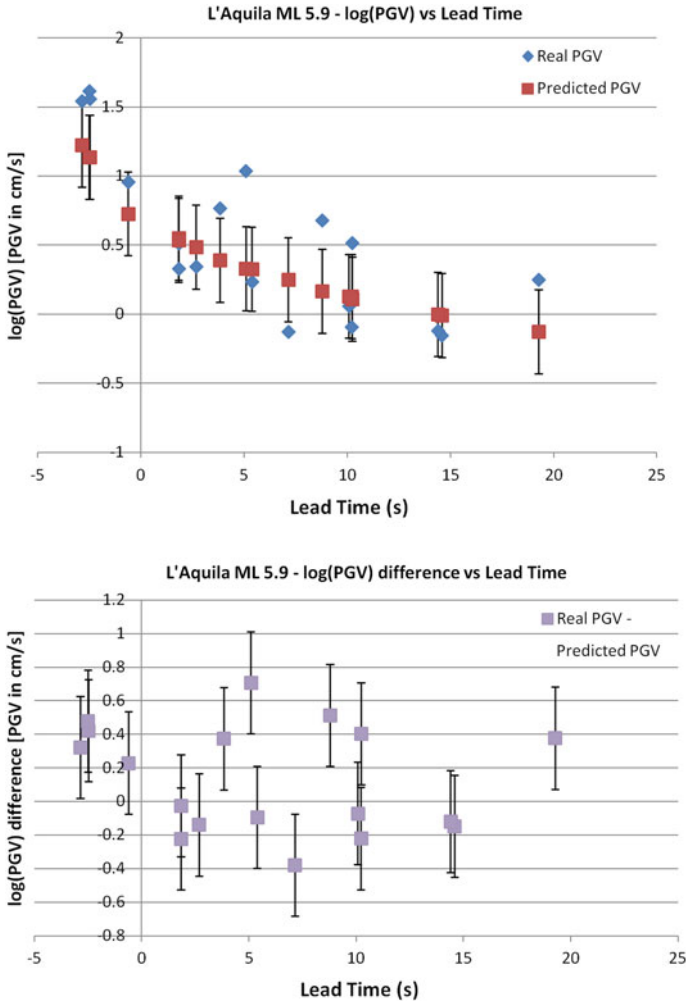


**Fig. 7.6** Play-back in PRESTo of the 2009 L'Aquila earthquake. *Top* distribution of measured (*blue diamonds*) and predicted (*red squares*) Peak Ground Velocities at RAN stations, as a function of lead-time. PGVs were predicted by PRESTo using the Akkar and Bommer (2007) GMPE. *Bottom* difference between measured and predicted PGVs. Error bars on the PRESTo estimates correspond to the standard deviation of the adopted GMPE

corresponding to  $P_d = 0.2$  cm) is expected to reproduce with a good approximation the area within which the highest intensity values are observed. For each of the analyzed earthquakes we compared the PDZ map with the instrumental intensity ( $I_{MM}$ ) and the Japanese intensity ( $I_{JMA}$ ) maps. Some examples of the results obtained are shown in Fig. 7.7. The simple visual comparison among the three maps shows that the real-time

**Table 7.2** Definition of successful, missed and false alarms

Recorded alert level	Successful alarm	Missed alarm	False alarm
3	$I_{MM} \geq VII$	n.d. <sup>a</sup>	$I_{MM} < VII$
2	$I_{MM} \geq VII$	n.d. <sup>a</sup>	$I_{MM} < VII$
1	$I_{MM} < VII$	$I_{MM} \geq VII$	n.d. <sup>a</sup>
0	$I_{MM} < VII$	$I_{MM} \geq VII$	n.d. <sup>a</sup>

Each recorded alert level corresponds to a successful, missed or false alarm, based on the observed values of intensity at the recording site. For example, a recorded alert level 3 corresponds to a successful alarm if the observed intensity is  $\geq VII$  and to a false alarm if the observed intensity is  $\leq VII$ . In the same way, the recorded alert level 1 can be a successful alarm if the observed intensity is  $< VII$  and a missed alarm if the observed intensity is  $\geq VII$ . The alert levels 3 or 2 cannot be missed alarms, as well as 1 and 0 cannot be false alarms

<sup>a</sup>n.d. not defined

PDZ is very consistent with the area in which the highest level of damage is reported, both on the  $I_{JMA}$  and  $I_{MM}$  maps.

A more robust strategy for a quantitative assessment of the system performance consists in evaluating the correspondence between the alert level issued at each station and the macroseismic intensity really experimented during the earthquake. To this end, we defined “successful”, “missed” and “false” alarms, based on the criteria listed in the Table 7.2. For example, according to the definition of alert level 3 (i.e.,  $P_d > 0.2$  cm), the instrumental intensity is expected to be greater than VII. Thus, a recorded alert level 3 corresponds to a successful alarm if the real observed intensity is larger than VII. On the other hand, it is considered a false alarm if the observed intensity is  $\leq VII$ . Similarly, the recorded alert level 1 corresponds to successful alarm if the observed intensity is less than VII, and to a missed alarms if the observed intensity is  $\geq VII$ .

To evaluate the system performance we then counted the total number of successful, missed and false alarms, according to the definitions given before. The main results are shown in Fig. 7.8: the 87.4 % of alert levels was correctly assigned, false alarms were the 11.9 % and missed alarms the 0.7 %. Despite the very high percentage of successful alarms, the percentage of false alarms turned out to be relatively high. In order to understand the relevance of this result we computed the difference between the predicted intensity ( $I_{MM} = VII$ ) and the real observed intensity value. The variance distribution represented in the left panel of Fig. 7.8 shows that the 52 % of the false alarms correspond to a real observed intensity equal to V. In this case the alert levels are obviously overestimated even if it should be noted that a value of V on the intensity scale is synonymous of an earthquake that can produce some damage. Thus, the 52 % of the false alarms were, in any case, not completely wrong.



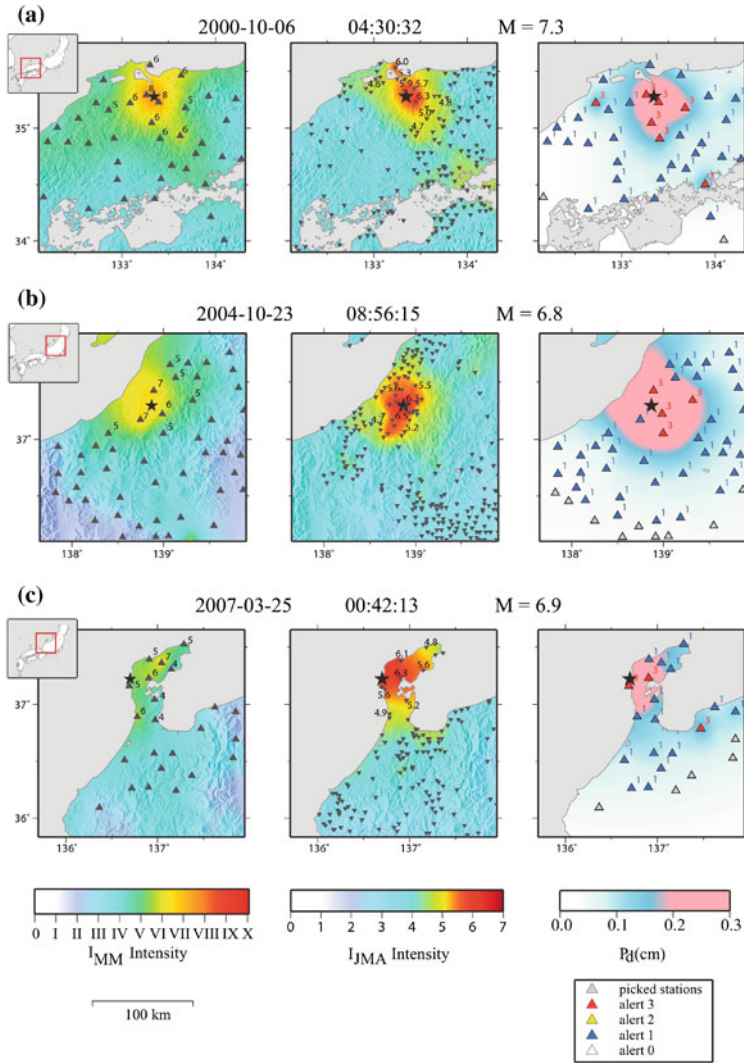


**Fig. 7.7** Examples of results for the threshold-based method for **a** M 7.3, 2007, Western Tottori earthquake, **b** M 6.8, 2004, Chuetsu earthquake and **c** M 6.9, 2007, Noto-Hanto earthquake. In each panel, the black star represents the epicenter and the triangles indicate the stations used for the analysis. Left panels.  $I_{MM}$  maps obtained from the observed PGV values at K-Net and Kik-Net stations. Values of measured PGV are reported for some stations in the epicentral area, as a reference. Center panels. The instrumental intensity,  $I_{JMA}$  maps, as measured at JMA sites are represented by the same color palette than the  $I_{MM}$  map, but adapted from 0 to 7. Values of instrumental intensity are reported for some stations in the epicentral area, as a reference. Right panels. the “operative early-warning map” resulting from the interpolation of measured and predicted  $P_d$  values. Triggered stations are represented by grey triangles, while red and blue triangles show the alert level recorded at each station, as soon as 3 seconds of signal after the P-picking are available. The PDZ is delimited by the color transition from light blue to red

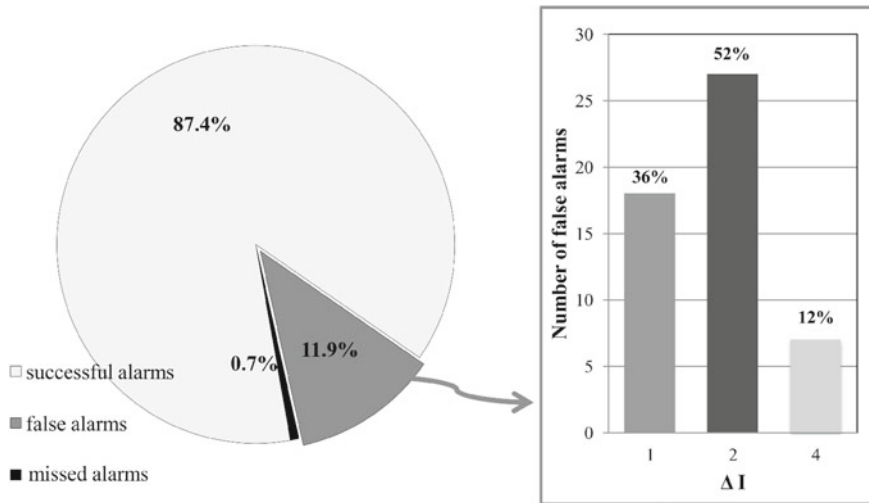


**Fig. 7.8** Cumulative statistic of successes/failures of the threshold-based system. *Left-side* relative percentage of successful, false and missed alarms, which are about 87, 11 and 0.7 %, respectively. *Right-side* histogram for the false alarms.  $\Delta I$  represents the difference between predicted ( $I_{MM} = VII$ ) and observed intensity values. 36 % of false alert levels 3 corresponds to an intensity value of VI; 52 % corresponds to intensity V and 12 % to intensity III

## 7.5 Conclusions

Most of the existing earthquake early-warning systems are either “regional” or “on-site”. A new concept is the integration of these approaches through the definition of alert levels and the real-time estimation of the earthquake Potential Damage Zone. In the regional approach the ground-motion parameters are computed only using earthquake location and magnitude; on the other hand, in a classical on-site approach the alert notification is based only on local ground-motion measurements. The integrated approach, instead, is based on the combined use of measured and predicted ground-motion parameters. Thus, it is likely to provide a more robust prediction of the potential earthquake damage effects.

The integrated approach is under development and testing in Southern Italy, using data streaming from the Irpinia Seismic Network. Here we presented the preliminary results of performance tests for the on-site and the regional method separately. The integrated approach will be tested off-line using moderate-to-strong earthquakes from worldwide catalogues.

### 7.5.1 Data and Resources

Waveforms used in this study have been extracted from ISNet database managed by AMRA Scarl (Analisi e Monitoraggio del Rischio Ambientale) and are available on-line at <http://seismnet.na.infn.it/index.jsp> after registration. Most of the analysis and figures were produced using GNUPLOT (<http://www.gnuplot.info/> last accessed January 2012), SAC (Goldstein et al. 2003) which can be requested from the Incorporated Research Institutions for Seismology (<http://www.iris.edu> last accessed January 2012), and GMT Generic Mapping Tools (Wessel and Smith 1995) (<http://gmt.soest.hawaii.edu/> last accessed January 2012). Details about the real-time seismological data transmission protocol SeedLink are available on-line at <http://www.iris.edu/data/dmc-seedlink.htm> (last accessed March 2012).

**Acknowledgments** This work was financially supported by Dipartimento della Protezione Civile (DPC) through Analisi e Monitoraggio del Rischio Ambientale (AMRA Scarl).

## References

- Akkar S, Bommer JJ (2007) Empirical prediction equations for peak ground velocity derived from strong-motions records from Europe and the Middle East. *Bull Seism Soc Am* 97:511–530
- Alcik H, Ozel O, Apaydin N, Erdik M (2009) A study on warning algorithms for Istanbul earthquake early warning system. *Geophys Res Lett* 36: L00B05. doi:10.1029/2008GL036659
- Allen RM, Kanamori H (2003) The potential for earthquake early warning in southern California. *Science* 300:685–848
- Allen RM, Brown H, Hellweg M, Khainovski O, Lombard P, Neuhauser D (2009a) Real-time earthquake detection and hazard assessment by ElarmS across California. *Geophys Res Lett* 36: L00B08. doi:10.1029/2008GL036766
- Allen RM, Gasparini P, Kamigaichi O, Böse M (2009b) The status of earthquake early warning around the world: an introductory overview. *Seism Res Lett* 80:682–693
- Allen RV (1978) Automatic earthquake recognition and timing from single traces. *Bull Seism Soc Am* 68:521–532
- Allen RV (1982) Automatic phase pickers: their present use and future prospects. *Bull Seism Soc Am* 72:225–242
- Baer M, Kradolfer U (1987) An automatic phase picker for local and teleseismic events. *Bull Seism Soc Am* 77:1437–1445
- Bagh S, Chiaraluce L, De Gori P, Moretti M, Govoni A, Chiarabba C, Di Bartolomeo P, Romanelli M (2007) Background seismicity in the central Apennines of Italy: the Abruzzo region case study. *Tectonophysics* 444:80–92. doi:10.1016/j.tecto.2007.08.009
- Böse M, Ionescu C, Wenzel F (2007) Earthquake early warning for Bucharest, Romania: novel and revised scaling relations. *Geophys Res Lett* 34. doi:10.1029/2007GL029396
- Böse M, Hauksson E, Solanki K, Kanamori H, Heaton TH (2009) Real-time testing of the on-site warning algorithm in Southern California and its performance during the July 29, 2008 Mw 5.4 Chino Hills earthquake. *Geophys Res Lett* 36. doi:10.1029/2008GL036366
- Cirella A, Piatanesi A, Cocco M, Tinti E, Scognamiglio L, Michelini A, Lomax A, Boschi E (2009) Rupture history of the 2009 L'Aquila (Italy) earthquake from non-linear joint inversion of strong motion and GPS data. *Geophys Res Lett* 36: L19304. doi:10.1029/2009GL039795
- Colombelli S, Amoroso O, Zollo A, Kanamori H (2012) Test of a threshold-based earthquake early-warning method using Japanese data. *Bull Seism Soc Am* 102. doi:10.1785/0120110149

- Emolo A, Convertito V, Cantore L (2011) Ground-motion predictive equations for low-magnitude earthquakes in the Campania-Lucania area, southern Italy. *J Geophys Eng* 8:46–60. doi:[10.1088/1742-2132/8/1/007](https://doi.org/10.1088/1742-2132/8/1/007)
- Espinosa-Aranda JM, Cuellar A, Garcia A, Ibarrola G, Islas R, Maldonado S, Rodriguez FH (2009) Evolution of the Mexican Seismic Alert System. *Seism Res Lett* 80:694–706
- Goldstein P, Dodge D, Firpoand M, Minner L (2003) SAC2000: Signal processing and analysis tools for seismologists and engineers. In: IASPEI international handbook of earthquake and engineering seismology
- Horiuchi S, Negishi N, Abe K, Kamimura K, Fujinawa Y (2005) An automatic processing system for broadcasting system earthquake alarms. *Bull Seism Soc Am* 95:347–353
- Iannaccone G, Zollo A, Elia L, Convertito V, Satriano C, Festa G, Martino C, Lancieri M, Bobbio A, Stabile TA, Vassallo M, Emolo A (2010) A prototype system for earthquake early-warning and alert management in southern Italy. *Bull Earthq Eng* 8:1105–1129. doi:[10.1007/s10518-009-9131-8](https://doi.org/10.1007/s10518-009-9131-8)
- Lancieri M, Zollo A (2008) A Bayesian approach to the real time estimation of magnitude from the early P-and S-wave displacement peaks. *J Geophys Res* 113(B12302). doi:[10.1029/2007JB005386](https://doi.org/10.1029/2007JB005386)
- Lomax A, Satriano C, Vassallo M (2012) Automatic picker developments and optimization: FilterPicker—a robust, broadband picker for real-time seismic monitoring and earthquake early-warning. *Seism Res Lett* 83(3):531–540. doi:[10.1785/gssrl.83.3.531](https://doi.org/10.1785/gssrl.83.3.531)
- Maercklin N, Zollo A, Orefice A, Festa G, Emolo A, De Matteis R, Delouis B, Bobbio A (2011) The effectiveness of a distant accelerometer array to compute seismic source parameters: the April 2009 L'Aquila earthquake case history. *Bull Seism Soc Am* 101:354–365. doi:[10.1785/0120100124](https://doi.org/10.1785/0120100124)
- Nakamura Y (1984) Development of earthquake early-warning system for the Shinkansen, some recent earthquake engineering research and practical in Japan. In: The Japanese national committee of the international association for earthquake engineering, pp 224–238
- Nakamura Y (1988) On the urgent earthquake detection and alarm system (UrEDAS). In: Proceedings of the 9th world conference earthquake engineering, vol 7, pp 673–678
- Odaka T, Ashiya K, Tsukada S, Sato S, Ohtake K, Nozaka D (2003) A new method of quickly estimating epicentral distance and magnitude from a single seismic record. *Bull Seism Soc Am* 93:526–532
- Peng HS, Wu ZL, Wu YM, Yu SM, Zhang DN, Huang WH (2011) Developing a prototype earthquake early warning system in the Beijing capital region. *Seism Res Lett* 82:394–403
- Satriano C, Lomax A, Zollo A (2008) Real-time evolutionary earthquake location for seismic early warning. *Bull Seism Soc Am* 98:1482–1494
- Satriano C, Elia L, Martino C, Lancieri M, Zollo A, Iannaccone G (2010) PRESto, the earthquake early warning system for southern Italy: concepts, capabilities and future perspectives. *Soil Dyn Earthq Eng*. doi:[10.1016/j.soildyn.2010.06.008](https://doi.org/10.1016/j.soildyn.2010.06.008)
- Wald DJ, Quitoriano V, Heaton TH, Kanamori H (1999) Relationships between peak ground acceleration, peak ground velocity and modified mercalli intensity in California. *Earthq Spectra* 15:557–564
- Wessel P, Smith WHF (1995) New version of the generic mapping tools released. *EOS Trans AGU* 76:329
- Wu YM, Kanamori H (2005) Rapid assessment of damage potential of earthquake in Taiwan from beginning of P waves. *Bull Seism Soc Am* 95:1181–1185. doi:[10.1785/0120040193](https://doi.org/10.1785/0120040193)
- Wu YM, Kanamori H (2008) Development of an earthquake early warning system using real-time strong motion signals. *Sensors* 8:1–9
- Wu YM, Teng LT (2002) A virtual sub-network approach to earthquake early warning. *Bull Seism Soc Am* 92:2008–2018
- Wu YM, Zhao L (2006) Magnitude estimation using the first three seconds P-wave amplitude in earthquake early warning. *Geophys Res Lett* 33:L16312. doi:[10.1029/2006GL026871](https://doi.org/10.1029/2006GL026871)

- Zollo A, Amoroso O, Lancieri M, Wu YM, Kanamori H (2010) A threshold-based earthquake early warning using dense accelerometer networks. *Geophys J Int* 183:963–974
- Zollo A, Iannaccone G, Convertito V, Elia L, Iervolino I, Lancieri M, Lomax A, Martino C, Satriano C, Weber E, Gasparini P (2009a) The earthquake early warning system in southern Italy. *Encyc Complex Syst Sci* 5:2395–2421. doi:[10.1007/978-0-387-30440-3](https://doi.org/10.1007/978-0-387-30440-3)
- Zollo A, Iannaccone G, Lancieri M, Cantore L, Convertito V, Emolo A, Festa G, Gallovič F, Vassallo M, Martino C, Satriano C, Gasparini P (2009b) Earthquake early warning system in southern Italy: methodologies and performance evaluation. *Geophys Res Lett* 36: L00B07. doi:[10.1029/2008GL03668](https://doi.org/10.1029/2008GL03668)